Title

Isoform- and Cell Type–Specific Roles of Glycogen Synthase Kinase 3 N-Terminal Serine Phosphorylation in Liver Ischemia Reperfusion Injury

Journal

The Journal of Immunology, 205(4)

ISSN

0022-1767

Authors

Ni, Ming
Zhou, Haoming
Zhang, Jing
et al.

Publication Date

2020-08-15

DOI

10.4049/jimmunol.2000397

Peer reviewed

HHS Public Access

Author manuscript

J Immunol. Author manuscript; available in PMC 2022 January 25.

Published in final edited form as:

J Immunol. 2020 August 15; 205(4): 1147–1156. doi:10.4049/jimmunol.2000397.

Isoform- and cell-type specific roles of Glycogen Synthase Kinase 3 N-terminal serine phosphorylation in liver ischemia reperfusion injury

Ming Ni[#,1,2], **Haoming Zhou**[#,1,2], **Jing Zhang**[1], **Dan Jin**[1,3], **Tianfei Lu**[1,4], **Ronald W. Busuttil**[1], **Jerzy W. Kupiec-Weglinski**[1], **Xuehao Wang**[2,*], **Yuan Zhai**[1,*]

[1]Dumont-UCLA Transplant Center, Division of Liver and Pancreas Transplantation, Department of Surgery, David Geffen School of Medicine at University of California-Los Angeles, Los Angeles, CA

[2]Department of Liver Surgery, The First Affiliated Hospital of Nanjing Medical University, Nanjing, Jiangsu Province, China

[3]Department of Obstetrics and Gynecology, Renji Hospital, Shanghai Jiaotong University, Shanghai, China

[4]Liver Surgery, Renji Hospital, Shanghai Jiaotong University, Shanghai, China

Abstract

Glycogen synthase kinase 3 (Gsk3) α and β are both constitutively active and inhibited upon stimulation by N-terminal serine phosphorylation. Although roles of active Gsk3 in liver ischemia reperfusion injury (IRI) have been well appreciated, whether Gsk3 N-terminal serine phosphorylation has any functional significance in the disease process remains unclear. In a murine liver partial warm ischemia model, we studied Gsk3-N-terminal serine mutant knock-in (KI) mice and showed that liver IRI was decreased in Gsk3αS21A, but increased in Gsk3βS9A, mutant KI mice. Bone marrow chimeric experiments revealed that the Gsk3α, but not β, mutation in liver parenchyma protected from IRI and both mutations in bone marrow-derived cells exacerbated liver injuries. Mechanistically, mutant Gsk3α protected hepatocytes from inflammatory (TNF-α) cell death by the activation of HIV-1 TAT-interactive protein 60 (TIP60)-mediated autophagy pathway. The pharmacological inhibition of TIP60 or autophagy diminished the protection of the Gsk3α mutant hepatocytes from inflammatory cell death in vitro and the Gsk3α mutant KI mice from liver IR injury in vivo. Thus, Gsk3 N-terminal serine phosphorylation inhibits liver innate immune activation but suppresses hepatocyte autophagy in response to inflammation. Gsk3 αS21, but not βS9, mutation is sufficient to sustain Gsk4 activities in hepatocytes and protect livers from IRI via TIP60 activation.

[*]**Corresponding authors:** Yuan Zhai, MD, PhD. Dumont-UCLA Transplant Center 77-120 CHS, 10833 Le Conte Ave, Los Angeles, CA 90095. Phone: (310) 825-9426; Fax: (310) 267-2367; yzhai@mednet.ucla.edu; Xuehao Wang, MD, Department of Liver Surgery, The First Affiliated Hospital of Nanjing Medical University, 300 Guanzhou Road, Nanjing, P.R.China. Phone: 86-25-68136053; Fax: 86-25-84630769; xhwang@njmu.edu.cn.

[#]M Ni and HM Zhou contribute equally to the work.

Introduction

Ischemia reperfusion injury (IRI) remains one of the primary causes of liver dysfunction and failure after hepatic tumor resection, liver transplantation, and trauma. Following the initial ischemic insult, reperfusion-triggered sterile inflammation is the major driving force of the disease pathogenesis. Host sentinel pattern recognition receptors are activated by danger associated molecular pattern, such as high mobility group box 1, derived from necrotic/stressed cells, resulting in production of inflammatory cytokines/chemokines by innate immune cells, including Kupffer cells (KC)/macrophages, dendritic cells and neutrophils (1, 2). These soluble mediators not only cause direct hepatocellular damage, but also recruit/activate more inflammatory cells from circulation into the tissue to amplify the immune response and tissue damage.

At the cellular level, Toll-Like-Receptor 4-mediated KC/macrophage activation and TNF-α-mediated hepatocyte/endothelium death are critical in the pathophysiology of liver IRI (3–8). In the exploration of regulatory mechanisms of these key processes, Glycogen synthase kinase 3β (Gsk3β) has attracted much attention, due to its ubiquitous expression pattern and indispensable roles in cell metabolism, proliferation, differentiation, and death (9–12). Gsk3β is a serine/threonine kinase and transduces signals downstream of both TLR4 and TNF-α. Distinctive from mitogen-activated protein kinases, Gsk3β differentially regulates pro- and anti-inflammatory cytokine gene transcriptions (10). Gsk3β also determine the sensitivity of hepatocyte response to TNF-α that global Gsk3β knock-out is lethal due to severe TNF-α toxicity in livers (13, 14). Additionally, Gsk3β has been found to regulate non-receptor mediated intrinsic cell death via the mitochondrial permeability transition pore (9, 15), which is critically involved in ischemia-induced cell death mechanism.

Gsk3 has two isoforms, α and β, which share extensive homology in the kinase domain, but are distinctive in their N- and C-terminals. The majority of Gsk3 research has been focused on the β isoform using small molecule inhibitors. However, these inhibitors actually do not discriminate between kinase domains of Gsk3 isoforms (16). Although Gsk3 isoforms have overlapping functions, isoform-specific properties have begun to reveal in recent studies. While global Gsk3β KO mice are embryonic lethal (13), Gsk3α KO mice are viable and “normal” (17). It has been shown in myocardial disease models that Gsk3 α and β played distinctive or even opposite functions (18–22).

Gsk3 is a unique intracellular signaling kinase that it is constitutively active in resting cells and inhibited by phosphorylation in response to various stimuli. The N-terminal phosphorylation of serine residues of Gsk3 α at Ser21 and β at Ser9 are the major mechanism of Gsk3 inactivation, which are induced in hearts and livers by IR (23, 24). Multiple intracellular signaling pathways can act on the serine site of Gsk3s. Among them, the PI3 kinase-Akt pathway triggered by growth factors/insulin and inflammation and the AMPK-mTOR-S6K pathway induced by nutrient/energy alterations are highly relevant to organ IRI. We have shown in our previous studies that PI3K inhibitor reduced liver IR-induced Gsk3β phosphorylation and increased liver IRI (24), while PTEN KO-induced PI3K activation had the opposite effect (25). Although experiments using Gsk3 inhibitors (24) or gene KO (26) have established their roles as active kinases, the functional

significance of Gsk3 inhibitory phosphorylation in disease pathogenesis remains elusive. Indeed, studies in heart diseases have documented that active Gsk3 and Gsk3 N-terminal serine phosphorylation may play distinctive roles in different aspects of disease mechanisms (27, 28) (22). Little is known about the functional significance of Gsk3 inhibitory phosphorylation in liver diseases.

In the current study, we took advantage of Gsk3 α or β N-terminal serine phosphorylation-resistant mutant (S21A/S9A) KI mice (11) and their bone marrow chimeras to determine the role of Gsk3 inhibitory phosphorylation in an isoform- and cell-type specific manner in sterile liver inflammatory tissue injury post IR.

Materials and Methods

Mice.

Gsk3 αS21A and βS9A double mutant (Alanine replaces Serine at position 21 or 9, resistant to inhibitory phosphorylation) knock-in were provided by Dr. Alessi DR of University of Dundee (MRC). We have re-derived them by crossing with WT C57BL/6 mice (Jackson Laboratory, Bar Harbor, ME). Mice were housed in the University of California-Los Angeles animal facility under specific pathogen-free conditions and received humane care, according to the criteria outlined in the “Guide for the Care and Use of Laboratory Animals” prepared by the National Academy of Sciences and published by the National Institutes of Health (NIH publication 86-023 revised 1985).

Genotyping of GSK3α21A and GSK3β9A mice was carried out by PCR of genomic DNA isolated from mouse ear or tail samples as described (29). Primers for GSK3α21A were: P1 (5’-3’ TTGAAGTGGCTGGTACTGG CTCTG) and P2 (5’-3’ GTGTGCTCCAGAGTAGTACCTAGC), resulting in a 271 bp product from the wild type allele and a 317 bp product from the mutant allele. Primers for GSK3β9A were: P3 (5’-3’ TCACTGGTCTAGGGGTGGTGGAAG) and P4 (5’-3’ GGAGTCAGTGACAACACTTAACTT), resulting in a 233 bp product from the wild type allele and a 352 bp product from the mutant allele.

Generation of chimeric mice.

Recipient mice were exposed to otherwise lethal 1000cGy from a Cesium source 6 h prior to receiving $2.5x10^6$ bone marrow cells by tail vein injection. The bone marrow cells were prepared under sterile conditions from the tibia and femur bones of donor mice. Recipient mice were monitored closely for the first two weeks to ensure the successful bone marrow engraftment. Four groups of chimeric mice were generated: WT mice that received either WT (WT-WT) or Mutant KI (KI-WT) bone marrow; or Mutant KI mice that received either WT (WT-KI) or KI (KI-KI) bone marrow. At 6-8 weeks post reconstitution, Liver NPCs were isolated from WT or Gsk3a/b mutant KI, or WT-KI or KI-WT chimeric mice. Genomic DNA was isolated. WT and mutant Gsk3a/b fragments were analyzed by PCR.

Model of liver partial warm IRI.

A murine model of partial liver warm IRI was used, as described (30). Male mice at 6-8 week-old were employed in our experiments. Briefly, after anesthesia with 2.5% isoflurane, mice were injected with heparin (100 mg/kg). A midline incision was made to expose the abdominal cavity, and an atraumatic clip was then used to interrupt the arterial and portal venous blood supply to the cephalad lobes of the liver. Mice were maintained anesthetized with isoflurane and placed in a designed warm container (HTP-1500 Heat Therapy Pump, Adroit Medical Systems, USA) to keep the temperature at 29°C. After 90 min of partial hepatic warm ischemia, the clip was removed, initiating liver reperfusion. Mice were sacrificed after 1, 6, or 24h post reperfusion. Sham controls underwent the same procedure, but without vascular occlusion. TIP60 inhibitor TH1834 (50mg/kg, Axon Medchem, Reston, VA) or autophagy inhibitor 3-Methyladenine (3-MA, 30mg/kg, Sigma, St. Luis, MO) or PBS (vehicle control) was administered intraperitoneally 1h prior to the onset of liver ischemia. Serum alanine aminotransferase (sALT) levels were measured by IDEXX Laboratories. Part of the liver specimens were fixed in 10% buffered formalin and embedded in paraffin. Liver sections (4μm) were stained with H&E. The severity of liver IRI was graded blindly using Suzuki's criteria on a scale from 0 to 4. No necrosis, congestion/centrilobular ballooning is given a score of 0, whereas severe congestion and >60% lobular necrosis is given a score of 4.

Primary hepatocytes isolation and cultures.

Mouse primary hepatocytes were isolated as follows: livers were perfused in situ via the portal vein with calcium- and magnesium-free HBSS, followed by 0.27% collagenase IV (Sigma). Perfused livers were dissected and teased through 70 μM nylon mesh cell strainers (BD Biosciences). Liver cells were suspended in 20 mL DMEM with 10% FBS and centrifuged at 50×g for 2 min. Decanted the supernatant and then added 20 mL 40% cold Percoll (Sigma, P1644) to each tube and mixed gently. Centrifuged at 150×g for 7 min. Removed the supernatant and wash cells with DMEM+10% FBS. Hepatocytes were suspended in plating medium (Williams E Medium with Hepatocyte Thawing and Plating Supplement Pack) and plated in Collagen type I-coated plates. After 3h culture, plating medium were replaced with maintenance medium (Williams E Medium with Hepatocyte Maintenance Supplement Pack) and cultured overnight.

For cell death experiments: hepatocytes isolated from WT or GSK3 KI mice were pretreated with Actinomycin D(50ng/mL) for 30 min or Thapsigargin(1μM) for 1h, followed by TNF-α (25 ng/mL) treatment for 12 hours, culture medium was collected for further analysis. GSK3 inhibitor SB216763 (10μM) and autophagy inhibitor 3-Methyladenine (5mM) was added 30 min prior to above treatment in some experiments. For autophagy flux study, Chloroquine (50μM) was added 1 hour prior to TNF-α stimulation. Cell death and survival were detected by LDH assay and CCK-8 assay (Biochain Institute, Hayward, CA) respectively according to manufactory instruction.

Fluorescence/Confocal Microscopy of hepatocyte autophagy.

CYTO-ID® Autophagy detection kit (Enzo Life Sciences, Farmingdale, NY) was used in our experiments. In brief, primary hepatocytes were seeded onto Nunc eight-well Permanox

Plastic chamber slides (ThermoFisher) at 50-70% confluence and cultured overnight. Hepatocytes were treated with either Thapsigargin (1μM), or H202 (100 μM), or TNF-α (25 ng/mL, R&D System) in the absence or presence of 10μM TIP60 inhibitor NU9056 (Tocris) for 6 hours. The treated cells were washed twice with 1X Assay buffer, followed by the incubation with 100 μL of Microscopy Dual Detection Reagent for 30 minutes at 37°C. The labeled cells were washed once with 1X Assay Buffer and fixed with 4% formaldehyde for 20 minutes. After 3 time wash with 1X Assay Buffer, a coverslip was placed on the microscope slide. Cells were analyzed by wide-field confocal microscopy with 400X magnification. A standard FITC filter set was used for imaging the autophagic signal, and a DAPI filter set for nuclear signal.

Quantitative RT-PCR.

Total RNA (2μg) was reverse-transcribed into cDNA using a SuperScript III First-Strand Synthesis System (Invitrogen, Carlsbad, CA). Quantitative PCR was performed using DNA Engine with 4 Detector (MJ Research, Waltham, MA). In a final reaction volume of 20 μl, the following were added: 1× SuperMix (Platinum SYBR Green qPCR Kit, Invitrogen), cDNA, and 0.5 mM of each primer. Amplification conditions were 50 °C for 2 min and 95 °C for 5 min, followed by 50 cycles of 95 °C for 15s and then 60 °C for 30s. Primers used to amplify specific mouse gene fragments were the same as described previously (31).

Western blot.

Liver tissue or cellular proteins were extracted with ice-cold lysis buffer (1% Triton X-100, 0.5% sodium deoxycholate, 0.1% SDS, 10% glycerol, 137mM sodium chloride, 20mM Tris, pH 7.4). Proteins (30 μg) were subjected to 12% SDS-PAGE electrophoresis and transferred to PVDF nitrocellulose membrane. Antibodies against Phospho-Gsk3a, Phospho-Gsk3b, Gsk3a, Gsk3b, LC3B, Phospho-TIP60 (Ser86), Phospho-AMPKa (Thr172), Phospho-p70 S6K (Thr389), b-actin (Cell Signaling Technology, Danvers, MA) were used for Western blot analysis. ImageJ 1.47v software was used to quantitate western blot bands.

Electron Microscope.

Fresh liver tissue blocks (1 mm3 in size) were fixed in 2% glutaraldehyde in PBS for 2 h, and post-fixed in 1% osmium tetroxide for 2 h. Samples were then dehydrated with an ascending series of alcohol before embedding. Ultrathin sections were cut and stained with lead citrate. Images were captured using a transmission electron microscope (HT7700, HITACHI).

Statistical analysis.

Results are shown as mean ± SD. Unpaired Student t-test were used for pairwise statistical analyses, with $p<0.05$ (two tailed) considered statistically significant.

Results

The Gsk3 αS21 but not βS9, mutation protects livers from IRI.

We have shown previously that ischemia induced a transient downregulation of N-terminal serine 9 phosphorylation of Gsk3b, followed by upregulation of its phosphorylation during reperfusion in livers by Western blot analysis (24). A similar phosphorylation pattern was found in Gsk3α S21 in IR livers (Fig. 1). To determine the functional significance of Gsk3 N-terminal phosphorylation in liver IRI, we compared Gsk3 αS21A or βS9A single and double mutant KI mice with their WT controls. Liver injury and inflammation were measured at 6h and 24h post reperfusion. The result showed that liver IRI was significantly decreased in α single and αβ double mutant KI, but increased in β single mutant KI, mice, as compared with WT controls. The sALT levels were significantly decreased, and liver histological architecture was preserved much better with lower Suzuki scores in the protected α mutant-containing KI mice, while opposite changes were observed in Gsk3β single mutant KI mice (Fig. 2a, b). Interestingly, liver expressions of inflammatory genes, including TNF-α, IL-6, IL-1β and CXCL10, were all up-regulated in these Gsk3 α and β mutant KI mice, regardless of liver injury levels (Fig. 2c). Thus, the Gsk3 α but not β, N-terminal mutation protects livers from IRI, despite that both these mutations promote liver inflammatory activation. The observation that Gsk3 α and β double mutant KI mice were protected from liver IRI, similar to Gsk3 α single mutant KI mice, indicates that the Gsk3 αS21A mutation is dominant in determining the liver susceptibility to IRI.

Gsk3 αS21A mutation plays distinctive roles in parenchymal vs. non-parenchymal cells in liver IRI.

The paradoxical effects of Gsk3αS21A mutation on liver inflammatory response and tissue injury suggest that its distinctive roles in liver parenchymal vs. non-parenchymal cells (NPC) upon IR-stress. To address this question, we created bone marrow chimeras by reconstituting lethally irradiated Gsk3α single mutant KI (WT-KI) or WT (KI-WT) recipient mice with either WT or Gsk3α single mutant KI bone marrows (BMs), respectively. Thus, Gsk3α mutation was present only in the parenchyma in WT-KI chimeras or in NPCs in KI-WT chimeras. The liver chimeric properties in reconstituted mice were confirmed by Gsk3α genotyping (Supp Fig.1). Liver IRI, measured at 6h post reperfusion, was decreased in WT-KI chimeras with reduced sALT levels and better-preserved liver histological architectures (lower Suzuki scores), as compared with WT-WT chimeric mice (Fig. 3a, b). Liver inflammatory gene levels were concomitantly lower in WT-KI chimeras (Fig. 3d). In contrast, KI-WT chimeric mice developed significantly more severe liver IRI with higher levels of sALT, worse damaged liver histological architecture (Suzuki scores) and upregulated intrahepatic pro-inflammatory gene expression, as compared with their WT-WT chimeric controls (Fig. 3a, b, c). Similar results were observed in the bone marrow chimeras of Gsk3 αS21A/βS9A double mutant KI mice (data not shown). Additionally, KC/macrophage depletion by clodronate-encapsulated liposomes did not abrogate the liver protective phenotype in Gsk3α mutant KI mice (Supp Fig.2), indicative of a parenchyma-dependent mechanism. In vitro TLR4 stimulation of either BMMs or KCs from these mutant KI mice resulted in higher levels of TNF-α and lower levels of IL-10 productions, as compared with their WT counterparts (Supp Fig.3). These results indicate that Gsk3αS21A

mutation plays distinctive roles in different types of liver cells against IR: it protects livers from IRI in parenchyma but enhances liver inflammatory activation and exacerbates hepatocellular damage in NPCs.

Gsk3 αS21A mutation protects hepatocytes from TNF-a cytotoxicity.

As TNF-α is the major inflammatory mediator of hepatocytotoxicity in liver IRI (6–8), we studied whether Gsk3 N-terminal serine phosphorylation regulated hepatocyte response against TNF-α in vitro, Primary hepatocytes from WT and Gsk3α or β mutant KI mice were incubated with TNF-α for 24hrs in the presence of actinomycin D and the cytotoxicity was quantitated by the LDH assay. Significantly lower levels of cell death were detected in Gsk3α but not β mutant KI hepatocytes, as compared with those in their WT counterparts (Fig. 4). To confirm that active Gsk3 kinase was responsible for the cytoprotection in Gsk3α mutant KI hepatocytes, we added Gsk3 inhibitor SB216763 in cell cultures. Indeed, Gsk3 inhibition increase hepatocyte cell death of the mutant type and abrogate the differences between mutant KI and WT hepatocytes in their response to TNF-a. To test whether autophagy was involved in the protection of Gsk3α mutant KI hepatocytes from inflammatory cell death, we added 3-metheladenine (3-MA) in the culture media. Indeed, inhibition of autophagy increased cell death of Gsk3α mutant KI, but not WT, hepatocytes in response to TNF-α (Fig. 4). Thus, Gsk3α S21A but not β S9A mutation prevents the inactivation of Gsk3 in TNF-α-stimulated hepatocytes and protects them from inflammatory cell death by possibly autophagy-mediated mechanism.

Gsk3 αS21A mutation promotes hepatocyte autophagy in response to inflammation.

To further dissect the protective mechanisms of Gsk3a N-terminal serine mutation in liver parenchyma against IRI, we measured hepatocyte autophagy in response to inflammation in vitro. Active Gsk3 has been shown to mediate autophagy induction upon nutrient- and growth factor-deprivation by phosphorylation and activation of TIP60 (at serine 86), an acetyltransferase which activates ULK1 to initiate autophagy. The activation of autophagy signaling pathways in primary hepatocytes upon TNF-α stimulation in vitro was analyzed by Western Blotting. TNF-a triggered Gsk3 N-terminal phosphorylation in both α and β isoforms in WT hepatocytes, but not in mutant KI cells (Fig. 5). To measure Gsk3 kinase activities, we analyzed glycogen synthase (GS) phosphorylation. The GS phosphorylation was maintained at a constant level in Gsk3α mutant KI cells, but gradually decreased in WT and the β mutant KI cells (Fig. 5), indicating that Gsk3α, but not β, N-terminal serine mutation prevented the inactivation of Gsk3 kinase activities in hepatocytes upon TNF-a stimulation. This resulted in significantly higher levels of LC3B II induction, TIP60 phosphorylation, AMPK phosphorylation (Thr172), and lower level S6K phosphorylation, in Gsk3 αS21A mutant KI cells, as compared with those in WT and βS9A mutant KI cells (Fig. 5). Autophagy flux (differences in LC3B II levels in the absence and presence of chloroquine (CQ) were also increased in Gsk3α mutant KI cells (data not shown). Thus, the N-terminal serine mutation of Gsk3α, but not β, enhanced the activation of autophagy signaling pathways in hepatocytes upon TNF-a stimulation.

To directly visualize hepatocyte autophagy, we used a cationic amphiphilic tracer (Cyto-ID), which labeled specifically autophagic vacuoles in viable cells. We tested hepatocyte

autophagy induced by TNF-a, as well as H_2O_2 and Thapsigargin (Tg), which simulated oxidative and ER stress in the mechanism of hepatocellular damage in liver IRI. Thus, WT and Gsk3αβ single or double mutant KI hepatocytes were incubated with either Tg or H_2O_2 or TNF-α for 6h, followed by the staining with Cyto-ID and DAPI. Confocal microscopy of these stained cells showed autophagic vacuoles as green fluorescent particles surrounding blue cell nuclei (DAPI). Clearly, Gsk3 α, but not β, mutant KI hepatocytes had formed significantly more autophagic vacuoles in response to TNF-a, but not Tg or H_2O_2 (Fig. 6a). To determine whether TIP60 was responsible for the enhanced autophagy induction in Gsk3α mutant KI hepatocytes, we added a chemical inhibitor of TIP60, NU9056 (32), in the cultures during TNF-a stimulation. Indeed, inhibition of TIP60 reduced numbers of autophagic vacuoles in both the α mutant KI and WT cells and abrogated the difference between these two types of cells (Fig. 6b). These results indicate that Gsk3α but not β N-terminal serine mutation facilitates autophagy induction in hepatocytes in response to the inflammatory stimulation.

Gsk3 αS21A mutation promotes liver autophagy in response to IR-stress.

To determine whether Gsk3α mutation protected livers from IRI by enhancing the autophagy induction, we analyzed autophagy-related proteins in IR livers by Western blotting. Levels of autophagy biomarker LC3B II, as well as phosphorylated TIP60 and AMPKα, were significantly higher, while the level of phosphorylated S6K (as a measurement of mTORC1 activities) was slightly lower, in Gsk3α but not β mutant KI livers, as compared with those in WT controls (Fig. 7).

To visualize hepatocyte autophagy in vivo in response to IR, we analyzed IR-liver tissue sections by electron microscopy (EM). No autophagosomes were detected in sham livers of both WT and Gsk3α KI mice. IR induced liver autophagy, which was further enhanced by the Gsk3α mutation, as evidenced by the higher numbers of autophagosomes in IR livers of Gsk3a KI mutant mice than those of WT controls (Fig. 8).

To determine the functional significance of autophagy induction and TIP60 activation in Gsk3α mutant KI mice against IR, we treated the mice with 3-MA or a newly developed TIP60 inhibitor TH1834 (33, 34) prior to the onset of liver ischemia. These treatments did not affect the severity of liver IRI in WT mice (35). However, both inhibitors resulted in significant increases of liver IRI in Gsk3α mutant KI mice, as evidenced by higher sALT levels and worse damaged liver histological architectures in the 3-MA- and TH1832- vs. vehicle control-treated Gsk3α mutant KI mice (Fig. 9). Liver EM results showed that the 3-MA treatment diminished the numbers of autophagosomes in IR livers of Gsk3α KI mutant mice (Fig. 8). These data indicated that the Gsk3α mutation protected livers from IRI by enhancing TIP60 activation and autophagy induction in hepatocytes.

Discussion

By taking advantage of genetic tools, we demonstrated, for the first time in a clinically relevant liver sterile tissue inflammatory disease model, that Gsk3 N-terminal serine phosphorylation was involved in both innate immune activation and parenchymal cell death in an isoform- and cell-type-specific manner. The N-terminal serine mutation of both

Gsk3α and β enhanced macrophage pro-inflammatory activation, while Gsk3αS21A but not Gsk3βS9A, mutation protected hepatocytes from inflammatory cell death and livers from IRI. The Gsk3α mutation enhanced the activation of multiple autophagy induction pathways in hepatocytes upon TNF-a stimulation that both TIP60 and AMPKα activating phosphorylation were increased with a simultaneous decrease in the mTOR1 activity. Inhibition of autophagy or TIP60 reversed the protective phenotype in vitro and in vivo in Gsk3α mutant KI cohorts. These results show that Gsk3 N-terminal serine phosphorylation plays active and important roles in the disease pathogenesis.

Unlike mitogen-activated protein kinases, Gsk3 is constitutively active in cells and inhibited upon inflammatory/stress stimulation via the N-terminal serine phosphorylation. Multiple kinase/phosphatase pathways are involved in the regulation of Gsk3 serine phosphorylation (36, 37). The PI3K-Akt-mediated Gsk3β S9 phosphorylation has been shown to inhibit pro-inflammatory activation (24, 26, 38). However, it has been difficult to precisely address the functional question of N-terminal serine phosphorylation of Gsk3 by using chemical inhibitors of its upstream kinases, due to the off-target effects and lack of Gsk3 isoform specificities in vivo. We have tested a PI3 kinase inhibitor, which was able to partially reduce Gsk3β S9 phosphorylation in livers upon IR and showed that it did resulted in the exaggeration of liver IRI but only under the mild ischemic condition (24). In this study, we confirm that the N-terminal serine phosphorylation of both Gsk3 isoforms inhibits innate immune activation. Interestingly, although local inflammatory activation by IR is enhanced in Gsk3αS21A mutant KI mice, livers are protected against IRI due to the protection of mutant hepatocytes from inflammatory cell death. It suggests that the hepatocyte phenotype is dominant in determining the outcome of the inflammation.

Gsk3 αS21A/βS9Adouble mutant KI mice were initially created by McManus et al to study insulin and Wnt signaling and they have normal development and growth without signs of metabolic disorder and insulin resistance (29). In the myocardial disease model, Gsk3αβ double mutant KI has been shown to protect against pathological hypertrophy induced by chronic adrenergic stimulation, maintaining cardiac function and attenuating interstitial fibrosis (39). However, its effects on chronic pathological hypertrophy after regional infarction was marginal, suggesting its disease context-specific roles (40). Gsk3βS9A single mutant KI mice exhibited attenuated, but Gsk3αS21A single mutant KI mice showed exacerbated, hypertrophy and heart failure in response to pressure overload (28). In cardiomyocyte-specific and -inducible Gsk3β KO mice, Gsk3β regulated post-MI remodeling, but played a minor role in the hypertrophic response to pressure overload (18). Thus, Gsk3 regulates myocardial injury and remodeling in isoform-specific, molecular form-specific (as active kinase or via its inhibitory phosphorylation process) and disease context-dependent manner.

Gsk3 inhibitors have been shown to alleviate tissue damages in in the models of myocardial infarction, stroke, and liver IRI (15, 41, 42). We have shown previously, in the same murine liver partial warm ischemia model, that Gsk3 inhibitor SB216763 protected livers from inflammatory tissue injury via an IL-10-mediated immune regulatory mechanism (24). Results in this study raise an obvious question regarding to the potential detrimental effect of Gsk3 inhibitors. Gsk3 has been shown to promote cell death caused by the mitochondrial

intrinsic apoptotic pathway, but inhibit the death receptor-mediated extrinsic apoptotic signaling pathway (9, 20, 21). Both these pathways are involved in the hepatocellular damage mechanism post IR. Our data shows that active Gsk3a increase hepatocyte autophagy in response to TNF-a, but not oxidative/ER stress.

An obvious question for us to answer next is why the cytoprotective effect of N-terminal serine mutation was only associated with Gsk3α but not β isoform. We tested GS phosphorylation in these two types of mutant cells, as an indication of Gsk3 kinase activities. Results show that Gsk3α, but not β, mutation sustained the kinase activity in hepatocytes upon TNF-a stimulation, indicating that Gsk3β was inactivated independent of S9-phosphorylation. Indeed, multiple types of post-translational modifications have been identified to regulate Gsk3 β, but not α, activities (43), including inhibitory serine 389 phosphorylation (44) and ADP-ribosylation (45). Additionally, GSK-3β can be citrullinated within its N-terminal domain by protein arginine deiminase 4 (PAD4) to promote its nuclear accumulation (46) and ubiquitinated at lysine 63 by the E3 ligase TNF receptor-associated factor 6 (TRAF6) for its assembly with TLR3 (47). Thus, the N-terminal serine mutation is only sufficient for Gsk3α but not Gsk3β, to avoid inactivation in TNF-a stimulated hepatocytes.

The role of autophagy in IRI is both complex and controversial (48, 49). Our own study in the same murine liver IRI model has shown that mild ischemia (30m) triggers autophagy to protect livers from IRI, while prolonged ischemia (90m) inhibits autophagy to facilitate liver IRI (35). Our current results reveal a novel regulatory pathway in hepatocytes in response to TNF-α that Gsk3 inhibitory phosphorylation downregulate autophagy, in part, by inactivating the TIP60-ULK1 pathway. Our results also reveal the potential involvement of AMPK and mTORC1 in protecting hepatocytes downstream of active Gsk3α (Fig. 10). It has been found in Gsk3α knock-out mice that mTORC1 activities are significantly increased, leading to impaired autophagy in the heart and fibroblasts (50).

Gsk3 can phosphorylate hypoxia-inducible factor (HIF) 1α directly (51), leading to its ubiquitinylation and degradation via F-box and WD protein Fbw7, independent of von HippelLindau (VHL) (52). Thus, Gsk3 N-terminal mutation may result in lower levels of HIF-1α in response to IR. It will be interesting to be determined whether HIF-1α or its other isoforms are involved downstream of Gsk3 α or β to regulate liver IRI (Fig. 10). HIFs are accumulated/upregulated in response to not only hypoxia, but also inflammatory stimuli, such as LPS and TNF-α (53–55). Although they are generally thought to promote autophagy/survival in cells in their adaptation to oxygen and nutrient deprivation, the in vivo effect of HIF inhibition or genetic inactivation on the disease process is context- and isoform-dependent. In a HepG2 tumor spheroid model, knock-down of one HIF isoform (1a or 2a) resulted in the upregulation of the other, leading to higher levels of autophagy and survival advantages in tumor cells (56). Although the genetic knock-out of prolyl hydroxylase domain enzyme 1 (PHD1), which regulates the stability of HIFs, protects livers from IRI in vivo and hepatocytes from simulated IR in vitro, knock-down of HIF-1α or 2a fails to increase hepatocyte death against IR (57). Additionally, HIF has been identified as a key regulator of macrophage activation/functions in tissue inflammation via its ability to metabolically reprogramming the cells (54, 58). HIF isoforms may play distinctive

roles to either facilitate or regulate macrophage pro-inflammatory responses. One recent study documents that HIF-2α protects acute liver injury by promoting IL-6 production in macrophages (59). Clearly, multiple immune regulatory genes regulated by HIFs, such as ecto-5'-nucleotidase (CD73) (60), can be involved in the regulation of tissue inflammatory response further downstream of the Gsk3-HIF pathway.

In summary, our results demonstrate in vivo the functional significance of Gsk3α and β N-terminal serine phosphorylation in sterile inflammatory tissue injury. The novel regulatory role of active Gsk3 in hepatocyte autophagy in response to inflammatory stimuli sheds a new light on the disease mechanism that Gsk3 N-terminal phosphorylation contributes to liver IRI by inhibiting TIP60-initiated hepatocyte autophagy. Thus, Gsk3 functions both as an active kinase and via its inhibitory phosphorylation in the pathogenesis of liver IRI. We must take into consideration its complex roles in the isoform- and cell-type specific manner to design safe and effective Gsk3-targeted therapy.

Supplementary Material

Refer to Web version on PubMed Central for supplementary material.

Acknowledgments

This work was supported by NIH Grants P01Al120944 (YZ and JKW), The Dumont Research Foundation, and grants from the National Nature Science Foundation of China 81600450, 81870448, 3193002 ((HZ, XW).

References

1. Kaczorowski DJ, Tsung A, and Billiar TR. 2009. Innate immune mechanisms in ischemia/reperfusion. Front Biosci (Elite Ed) 1: 91–98. [PubMed: 19482628]
2. Zhai Y, Busuttil RW, and Kupiec-Weglinski JW. 2011. Liver ischemia and reperfusion injury: new insights into mechanisms of innate-adaptive immune-mediated tissue inflammation. American journal of transplantation : official journal of the American Society of Transplantation and the American Society of Transplant Surgeons 11: 1563–1569.
3. Tsung A, Hoffman RA, Izuishi K, Critchlow ND, Nakao A, Chan MH, Lotze MT, Geller DA, and Billiar TR. 2005. Hepatic ischemia/reperfusion injury involves functional TLR4 signaling in nonparenchymal cells. J Immunol 175: 7661–7668. [PubMed: 16301676]
4. Zhai Y, Shen X. d., O'Connell R, Gao F, Lassman C, Busuttil RW, Cheng G, and Kupiec-Weglinski JW. 2004. Cutting Edge: TLR4 Activation Mediates Liver Ischemia/Reperfusion Inflammatory Response via IFN Regulatory Factor 3-Dependent MyD88-Independent Pathway. The Journal of Immunology 173: 7115–7119. [PubMed: 15585830]
5. Wu HS, Zhang JX, Wang L, Tian Y, Wang H, and Rotstein O. 2004. Toll-like receptor 4 involvement in hepatic ischemia/reperfusion injury in mice. Hepatobiliary Pancreat Dis Int 3: 250–253. [PubMed: 15138120]
6. Colletti LM, Remick DG, Burtch GD, Kunkel SL, Strieter RM, and Campbell DA Jr. 1990. Role of tumor necrosis factor-alpha in the pathophysiologic alterations after hepatic ischemia/reperfusion injury in the rat. The Journal of clinical investigation 85: 1936–1943. [PubMed: 2161433]
7. Teoh N, Field J, Sutton J, and Farrell G. 2004. Dual role of tumor necrosis factor-alpha in hepatic ischemia-reperfusion injury: studies in tumor necrosis factor-alpha gene knockout mice. Hepatology 39: 412–421. [PubMed: 14767994]
8. Rudiger HA, and Clavien PA. 2002. Tumor necrosis factor alpha, but not Fas, mediates hepatocellular apoptosis in the murine ischemic liver. Gastroenterology 122: 202–210. [PubMed: 11781294]

9. Beurel E, and Jope RS. 2006. The paradoxical pro- and anti-apoptotic actions of GSK3 in the intrinsic and extrinsic apoptosis signaling pathways. Progress in neurobiology 79: 173–189. [PubMed: 16935409]
10. Beurel E, Michalek SM, and Jope RS. 2010. Innate and adaptive immune responses regulated by glycogen synthase kinase-3 (GSK3). Trends Immunol 31: 24–31. [PubMed: 19836308]
11. McManus EJ, Sakamoto K, Armit LJ, Ronaldson L, Shpiro N, Marquez R, and Alessi DR. 2005. Role that phosphorylation of GSK3 plays in insulin. Embo J 24: 1571–1583. [PubMed: 15791206]
12. Cohen P, and Goedert M. 2004. GSK3 inhibitors: development and therapeutic potential. Nat Rev Drug Discov 3: 479–487. [PubMed: 15173837]
13. Hoeflich KP, Luo J, Rubie EA, Tsao MS, Jin O, and Woodgett JR. 2000. Requirement for glycogen synthase kinase-3beta in cell survival and NF-kappaB activation. Nature 406: 86–90. [PubMed: 10894547]
14. Schwabe RF, and Brenner DA. 2002. Role of glycogen synthase kinase-3 in TNF-alpha-induced NF-kappaB activation and apoptosis in hepatocytes. American journal of physiology. Gastrointestinal and liver physiology 283: G204–211. [PubMed: 12065308]
15. Gomez L, Paillard M, Thibault H, Derumeaux G, and Ovize M. 2008. Inhibition of GSK3beta by postconditioning is required to prevent opening of the mitochondrial permeability transition pore during reperfusion. Circulation 117: 2761–2768. [PubMed: 18490522]
16. Avrahami L, Licht-Murava A, Eisenstein M, and Eldar-Finkelman H. 2013. GSK-3 inhibition: achieving moderate efficacy with high selectivity. Biochim Biophys Acta 1834: 1410–1414. [PubMed: 23369789]
17. MacAulay K, Doble BW, Patel S, Hansotia T, Sinclair EM, Drucker DJ, Nagy A, and Woodgett JR. 2007. Glycogen synthase kinase 3alpha-specific regulation of murine hepatic glycogen metabolism. Cell metabolism 6: 329–337. [PubMed: 17908561]
18. Woulfe KC, Gao E, Lal H, Harris D, Fan Q, Vagnozzi R, DeCaul M, Shang X, Patel S, Woodgett JR, Force T, and Zhou J. 2010. Glycogen synthase kinase-3beta regulates post-myocardial infarction remodeling and stress-induced cardiomyocyte proliferation in vivo. Circulation research 106: 1635–1645. [PubMed: 20360256]
19. Lal H, Zhou J, Ahmad F, Zaka R, Vagnozzi RJ, Decaul M, Woodgett J, Gao E, and Force T. 2012. Glycogen synthase kinase-3α limits ischemic injury, cardiac rupture, post-myocardial infarction remodeling and death. Circulation 125: 65–75. [PubMed: 22086876]
20. Juhaszova M, Zorov DB, Kim SH, Pepe S, Fu Q, Fishbein KW, Ziman BD, Wang S, Ytrehus K, Antos CL, Olson EN, and Sollott SJ. 2004. Glycogen synthase kinase-3beta mediates convergence of protection signaling to inhibit the mitochondrial permeability transition pore. The Journal of clinical investigation 113: 1535–1549. [PubMed: 15173880]
21. Juhaszova M, Zorov DB, Yaniv Y, Nuss HB, Wang S, and Sollott SJ. 2009. Role of glycogen synthase kinase-3beta in cardioprotection. Circ Res 104: 1240–1252. [PubMed: 19498210]
22. Lal H, Ahmad F, Woodgett J, and Force T. 2015. The GSK-3 family as therapeutic target for myocardial diseases. Circ Res 116: 138–149. [PubMed: 25552693]
23. Vigneron F, Dos Santos P, Lemoine S, Bonnet M, Tariosse L, Couffinhal T, Duplaa C, and Jaspard-Vinassa B. 2011. GSK-3beta at the crossroads in the signalling of heart preconditioning: implication of mTOR and Wnt pathways. Cardiovascular research 90: 49–56. [PubMed: 21233250]
24. Ren F, Duan Z, Cheng Q, Shen X, Gao F, Bai L, Liu J, Busuttil RW, Kupiec-Weglinski JW, and Zhai Y. 2011. Inhibition of glycogen synthase kinase 3 beta ameliorates liver ischemia reperfusion injury by way of an interleukin-10-mediated immune regulatory mechanism. Hepatology 54: 687–696. [PubMed: 21567437]
25. Yue S, Rao J, Zhu J, Busuttil RW, Kupiec-Weglinski JW, Lu L, Wang X, and Zhai Y. 2014. Myeloid PTEN deficiency protects livers from ischemia reperfusion injury by facilitating M2 macrophage differentiation. J Immunol 192: 5343–5353. [PubMed: 24771857]
26. Zhou H, Wang H, Ni M, Yue S, Xia Y, Busuttil RW, Kupiec-Weglinski JW, Lu L, Wang X, and Zhai Y. 2018. Glycogen synthase kinase 3β promotes liver innate immune activation by restraining AMP-activated protein kinase activation. Journal of hepatology 69: 99–109. [PubMed: 29452207]

27. Antos CL, McKinsey TA, Frey N, Kutschke W, McAnally J, Shelton JM, Richardson JA, Hill JA, and Olson EN. 2002. Activated glycogen synthase-3 beta suppresses cardiac hypertrophy in vivo. Proc Natl Acad Sci U S A 99: 907–912. [PubMed: 11782539]

28. Matsuda T, Zhai P, Maejima Y, Hong C, Gao S, Tian B, Goto K, Takagi H, Tamamori-Adachi M, Kitajima S, and Sadoshima J. 2008. Distinct roles of GSK-3alpha and GSK-3beta phosphorylation in the heart under pressure overload. Proc Natl Acad Sci U S A 105: 20900–20905. [PubMed: 19106302]

29. McManus EJ, Sakamoto K, Armit LJ, Ronaldson L, Shpiro N, Marquez R, and Alessi DR. 2005. Role that phosphorylation of GSK3 plays in insulin and Wnt signalling defined by knockin analysis. The EMBO journal 24: 1571–1583. [PubMed: 15791206]

30. Shen XD, Ke B, Zhai Y, Amersi F, Gao F, Anselmo DM, Busuttil RW, and Kupiec-Weglinski JW. 2002. CD154-CD40 T-cell costimulation pathway is required in the mechanism of hepatic ischemia/reperfusion injury, and its blockade facilitates and depends on heme oxygenase-1 mediated cytoprotection. Transplantation 74: 315–319. [PubMed: 12177608]

31. Zhai Y, Shen XD, Gao F, Zhao A, Freitas MC, Lassman C, Luster AD, Busuttil RW, and Kupiec-Weglinski JW. 2008. CXCL10 regulates liver innate immune response against ischemia and reperfusion injury. Hepatology 47: 207–214. [PubMed: 18041715]

32. Coffey K, Blackburn TJ, Cook S, Golding BT, Griffin RJ, Hardcastle IR, Hewitt L, Huberman K, McNeill HV, Newell DR, Roche C, Ryan-Munden CA, Watson A, and Robson CN. 2012. Characterisation of a Tip60 specific inhibitor, NU9056, in prostate cancer. PLoS One 7: e45539. [PubMed: 23056207]

33. Idrissou M, Judes G, Daures M, Sanchez A, El Ouardi D, Besse S, Degoul F, Penault-Llorca F, Bignon YJ, and Bernard-Gallon D. 2019. TIP60 Inhibitor TH1834 Reduces Breast Cancer Progression in Xenografts in Mice. OMICS 23: 457–459. [PubMed: 31487234]

34. Gao C, Bourke E, Scobie M, Famme MA, Koolmeister T, Helleday T, Eriksson LA, Lowndes NF, and Brown JA. 2014. Rational design and validation of a Tip60 histone acetyltransferase inhibitor. Scientific reports 4: 5372. [PubMed: 24947938]

35. Zhou H, Zhu J, Yue S, Lu L, Busuttil RW, Kupiec-Weglinski JW, Wang X, and Zhai Y. 2016. The Dichotomy of Endoplasmic Reticulum Stress Response in Liver Ischemia-Reperfusion Injury. Transplantation 100: 365–372. [PubMed: 26683513]

36. Kaidanovich-Beilin O, and Woodgett JR. 2011. GSK-3: Functional Insights from Cell Biology and Animal Models. Front Mol Neurosci 4: 40. [PubMed: 22110425]

37. Beurel E, Grieco SF, and Jope RS. 2015. Glycogen synthase kinase-3 (GSK3): regulation, actions, and diseases. Pharmacol Ther 148: 114–131. [PubMed: 25435019]

38. Martin M, Rehani K, Jope RS, and Michalek SM. 2005. Toll-like receptor-mediated cytokine production is differentially regulated by glycogen synthase kinase 3. Nat Immunol 6: 777–784. [PubMed: 16007092]

39. Webb IG, Nishino Y, Clark JE, Murdoch C, Walker SJ, Makowski MR, Botnar RM, Redwood SR, Shah AM, and Marber MS. 2010. Constitutive glycogen synthase kinase-3alpha/beta activity protects against chronic beta-adrenergic remodelling of the heart. Cardiovascular research 87: 494–503. [PubMed: 20299330]

40. Webb IG, Sicard P, Clark JE, Redwood S, and Marber MS. 2010. Myocardial stress remodelling after regional infarction is independent of glycogen synthase kinase-3 inactivation. Journal of molecular and cellular cardiology 49: 897–900. [PubMed: 20696171]

41. Ren M, Senatorov VV, Chen RW, and Chuang DM. 2003. Postinsult treatment with lithium reduces brain damage and facilitates neurological recovery in a rat ischemia/reperfusion model. Proc Natl Acad Sci U S A 100: 6210–6215. [PubMed: 12732732]

42. Fu H, Xu H, Chen H, Li Y, Li W, Zhu Q, Zhang Q, Yuan H, Liu F, Wang Q, Miao M, and Shi X. 2014. Inhibition of glycogen synthase kinase 3 ameliorates liver ischemia/reperfusion injury via an energy-dependent mitochondrial mechanism. J Hepatol 61: 816–824. [PubMed: 24862449]

43. Cormier KW, and Woodgett JR. 2017. Recent advances in understanding the cellular roles of GSK-3. F1000Res 6.

44. Thornton TM, Delgado P, Chen L, Salas B, Krementsov D, Fernandez M, Vernia S, Davis RJ, Heimann R, Teuscher C, Krangel MS, Ramiro AR, and Rincon M. 2016. Inactivation of nuclear

GSK3beta by Ser(389) phosphorylation promotes lymphocyte fitness during DNA double-strand break response. Nat Commun 7: 10553. [PubMed: 26822034]

45. Feijs KL, Kleine H, Braczynski A, Forst AH, Herzog N, Verheugd P, Linzen U, Kremmer E, and Luscher B. 2013. ARTD10 substrate identification on protein microarrays: regulation of GSK3beta by mono-ADP-ribosylation. Cell communication and signaling : CCS 11: 5. [PubMed: 23332125]
46. Stadler SC, Vincent CT, Fedorov VD, Patsialou A, Cherrington BD, Wakshlag JJ, Mohanan S, Zee BM, Zhang X, Garcia BA, Condeelis JS, Brown AM, Coonrod SA, and Allis CD. 2013. Dysregulation of PAD4-mediated citrullination of nuclear GSK3beta activates TGF-beta signaling and induces epithelial-to-mesenchymal transition in breast cancer cells. Proc Natl Acad Sci U S A 110: 11851–11856. [PubMed: 23818587]
47. Ko R, Park JH, Ha H, Choi Y, and Lee SY. 2015. Glycogen synthase kinase 3beta ubiquitination by TRAF6 regulates TLR3-mediated pro-inflammatory cytokine production. Nat Commun 6: 6765. [PubMed: 25828701]
48. Przyklenk K, Dong Y, Undyala VV, and Whittaker P. 2012. Autophagy as a therapeutic target for ischaemia/reperfusion injury? Concepts, controversies, and challenges. Cardiovascular research 94: 197–205. [PubMed: 22215722]
49. Gottlieb RA, and Mentzer RM. 2010. Autophagy during cardiac stress: joys and frustrations of autophagy. Annu Rev Physiol 72: 45–59. [PubMed: 20148666]
50. Zhou J, Freeman TA, Ahmad F, Shang X, Mangano E, Gao E, Farber J, Wang Y, Ma XL, Woodgett J, Vagnozzi RJ, Lal H, and Force T. 2013. GSK-3alpha is a central regulator of age-related pathologies in mice. The Journal of clinical investigation 123: 1821–1832. [PubMed: 23549082]
51. Flugel D, Gorlach A, Michiels C, and Kietzmann T. 2007. Glycogen synthase kinase 3 phosphorylates hypoxia-inducible factor 1alpha and mediates its destabilization in a VHL-independent manner. Mol Cell Biol 27: 3253–3265. [PubMed: 17325032]
52. Flugel D, Gorlach A, and Kietzmann T. 2012. GSK-3beta regulates cell growth, migration, and angiogenesis via Fbw7 and USP28-dependent degradation of HIF-1alpha. Blood 119: 1292–1301. [PubMed: 22144179]
53. Lee P, Chandel NS, and Simon MC. 2020. Cellular adaptation to hypoxia through hypoxia inducible factors and beyond. Nat Rev Mol Cell Biol 21: 268–283. [PubMed: 32144406]
54. Eltzschig HK, Bratton DL, and Colgan SP. 2014. Targeting hypoxia signalling for the treatment of ischaemic and inflammatory diseases. Nature reviews. Drug discovery 13: 852–869. [PubMed: 25359381]
55. Hellwig-Bürgel T, Rutkowski K, Metzen E, Fandrey J, and Jelkmann W. 1999. Interleukin-1beta and tumor necrosis factor-alpha stimulate DNA binding of hypoxia-inducible factor-1. Blood 94: 1561–1567. [PubMed: 10477681]
56. Menrad H, Werno C, Schmid T, Copanaki E, Deller T, Dehne N, and Brüne B. 2010. Roles of hypoxia-inducible factor-1alpha (HIF-1alpha) versus HIF-2alpha in the survival of hepatocellular tumor spheroids. Hepatology (Baltimore, Md.) 51: 2183–2192.
57. Schneider M, Van Geyte K, Fraisl P, Kiss J, Aragonés J, Mazzone M, Mairbäurl H, De Bock K, Jeoung NH, Mollenhauer M, Georgiadou M, Bishop T, Roncal C, Sutherland A, Jordan B, Gallez B, Weitz J, Harris RA, Maxwell P, Baes M, Ratcliffe P, and Carmeliet P. 2010. Loss or silencing of the PHD1 prolyl hydroxylase protects livers of mice against ischemia/reperfusion injury. Gastroenterology 138.
58. Lin N, and Simon MC. 2016. Hypoxia-inducible factors: key regulators of myeloid cells during inflammation. The Journal of clinical investigation 126: 3661–3671. [PubMed: 27599290]
59. Gao RY, Wang M, Liu Q, Feng D, Wen Y, Xia Y, Colgan SP, Eltzschig HK, and Ju C. 2019. Hypoxia-Inducible Factor-2α Reprograms Liver Macrophages to Protect Against Acute Liver Injury Through the Production of Interleukin-6. Hepatology (Baltimore, Md.).
60. Hart ML, Much C, Gorzolla IC, Schittenhelm J, Kloor D, Stahl GL, and Eltzschig HK. 2008. Extracellular adenosine production by ecto-5'-nucleotidase protects during murine hepatic ischemic preconditioning. Gastroenterology 135.

Key Points

Active Gsk3 promotes hepatocyte autophagy in response to TNF-α.

Gsk3 N-terminal phosphorylation inhibits macrophage TLR activation.

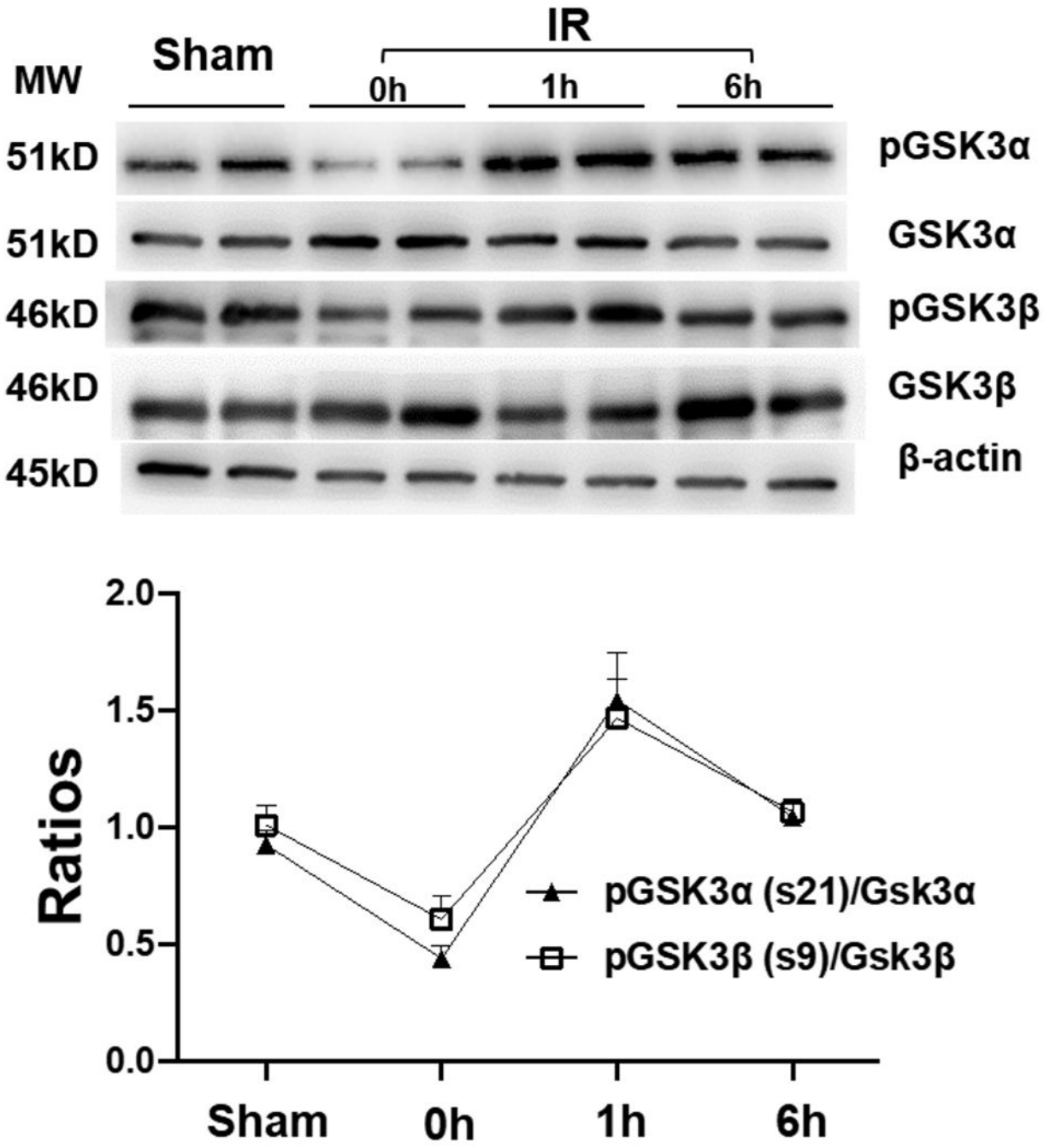

Figure 1:

Liver Gsk3 α and β N-terminal serine phosphorylation profiles in response to IR. Liver tissues were harvested after 90m ischemia and 0-, 1-, or 6-hour reperfusion, as described in the Materials and Methods. Total tissue proteins were analyzed by Western blots with anti-phosphorylated Gsk3αS21, Gsk3βS9, total Gsk3 α and β and β-actin antibodies (upper panel). Average ratios of phosphorylated vs. total Gsk3 α and β were plotted (lower panel). Representative results of 2 independent experiments.

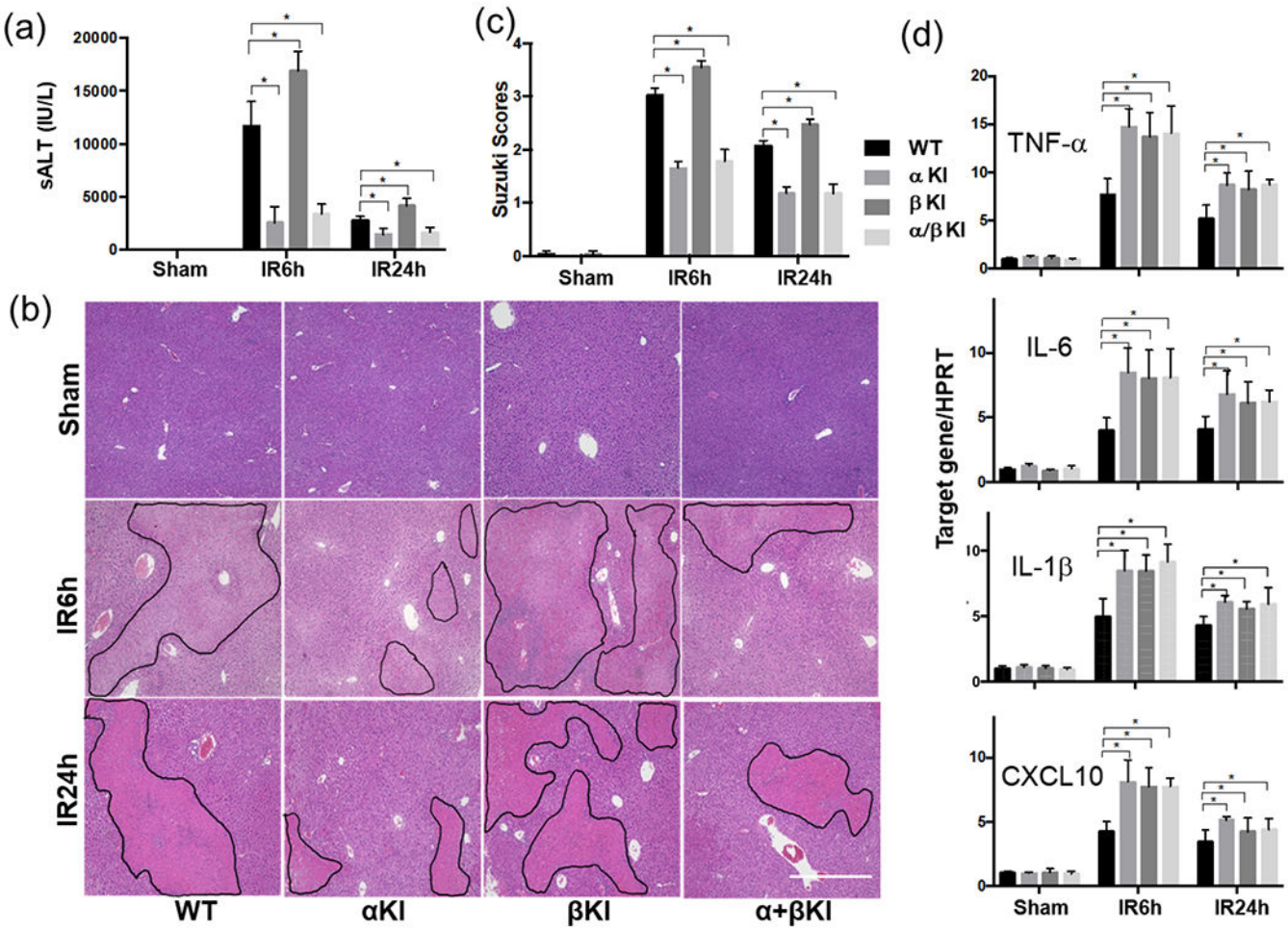

Figure 2:

Liver IRI in Gsk3αS21A and/or Gsk3βS9A single and double mutant KI mice. WT and Gsk3 mutant KI mice were subjected to liver IR experiments, as described in the Materials and Methods. Liver IRI and inflammatory responses were evaluated at both 6h and 24h post reperfusion. (a) Average sALT levels and Suzuki scores of different experimental groups; (b) Representative liver histological pictures (Scale bar=200μM), (c) Average gene expression levels (ratios of target gene/HPRT) of different experiment groups. n=4-6/group. Representative results of 2 separate experiments. *p<0.05

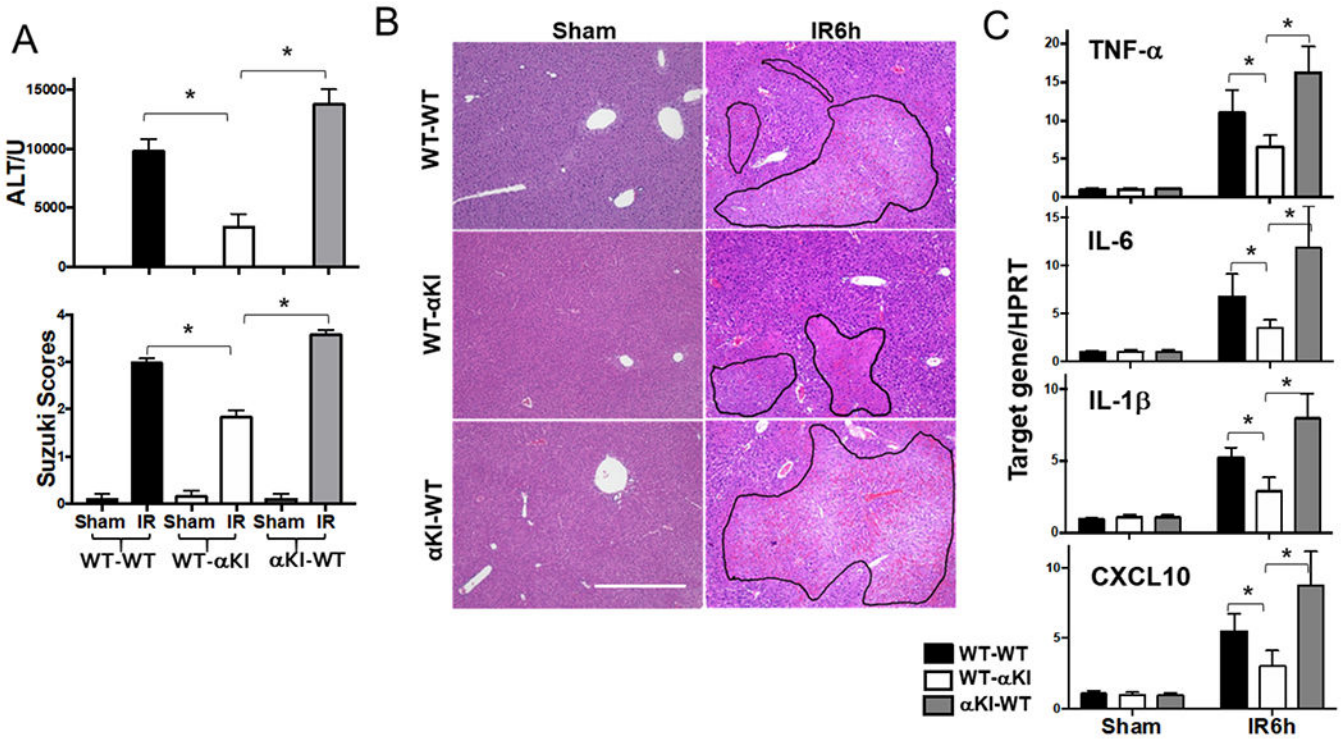

Figure 3:

Liver IRI in Gsk3αS21A mutant KI bone marrow chimeric mice. WT or Gsk3α mutant KI bone marrow chimeric mice, including WT-WT, WT-αKI, and αKI-WT, were generated and subjected to liver IR experiments, as described in the Materials and Methods. Liver injuries and inflammatory responses were evaluated at 6h post reperfusion. (a) Average sALT levels and Suzuki scores of different experimental groups, (b) Representative liver histological pictures, (Scale bar=200μM) (c) Average levels of inflammatory cytokine/chemokine gene expressions (ratios of target gene/HPRT) in different experimental groups. n=4-6/group. Representative results of 2 separate experiments. *$p<0.05$

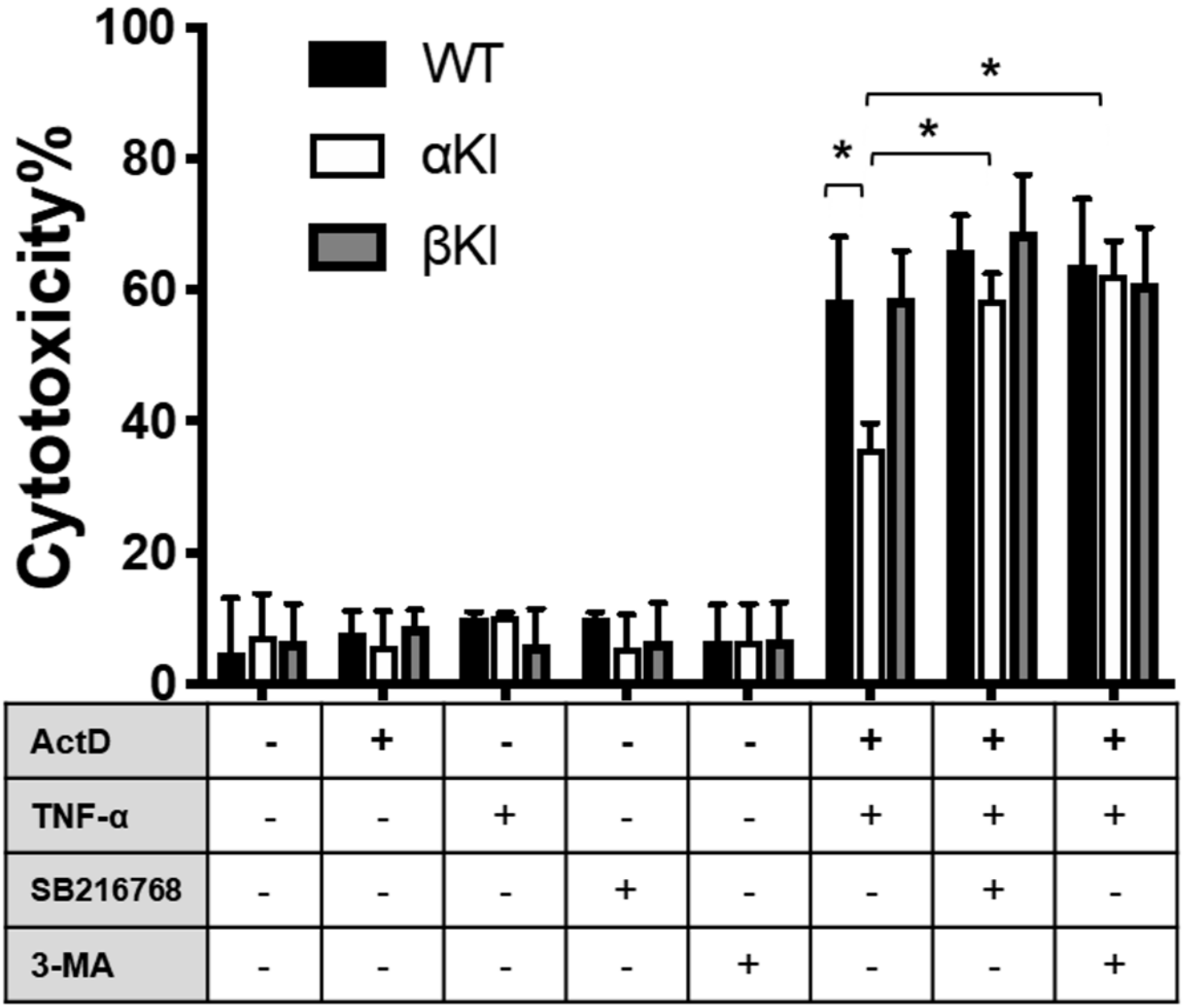

Figure 4:

TNF-α cytotoxicity in primary hepatocytes. Primary hepatocytes were isolated from WT and Gsk3α or β mutant KI mice, as described in the Materials and Methods. Cytotoxicity was induced by incubating cells with TNF-α in the presence of actinomycin D (ActD). Cell death was measured by LDH assay. Gsk3 inhibitor SB216763 or autophagy inhibitor 3-MA were added prior to the addition of ActD/TNF-α. Average percentages of cell death of different experimental groups were plotted. Representative results of at least 3 experiments. *$p<0.05$

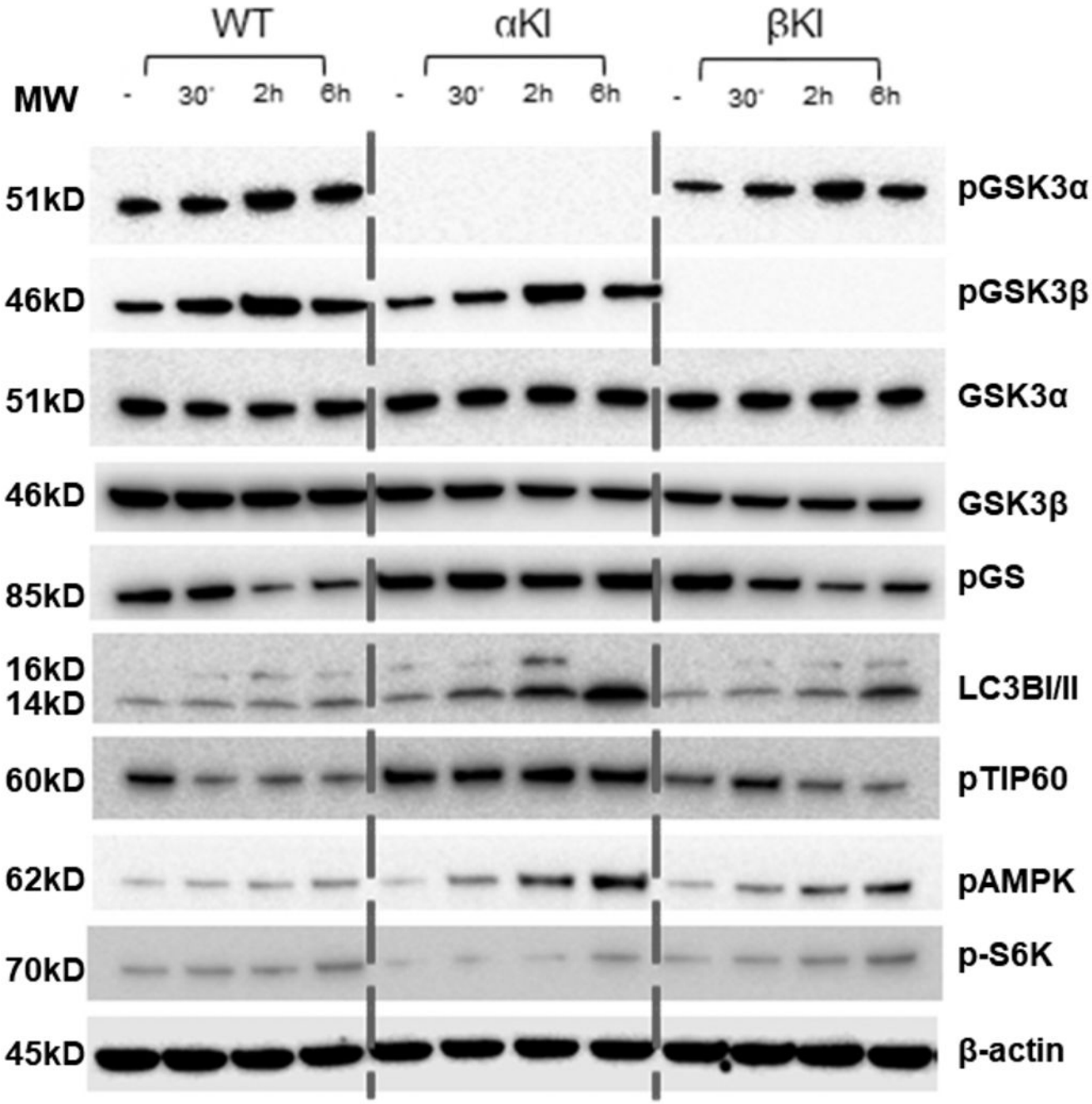

Figure 5:

Autophagy signaling pathways in primary hepatocytes in response to TNF-α. Primary hepatocytes were isolated from WT and Gsk3 α and β mutant KI mice, as described in the Materials and Methods. Cells were either unstimulated (-) or stimulated with TNF-α for 30m, 2h and 6h. Total cellular proteins were prepared and analyzed by Western blotting. Representative Western blots of phosphorylated forms and/or total of Gsk3α/β, TIP60, AMPK, S6K and LC3B I/II. Representative results of 3 independent experiments.

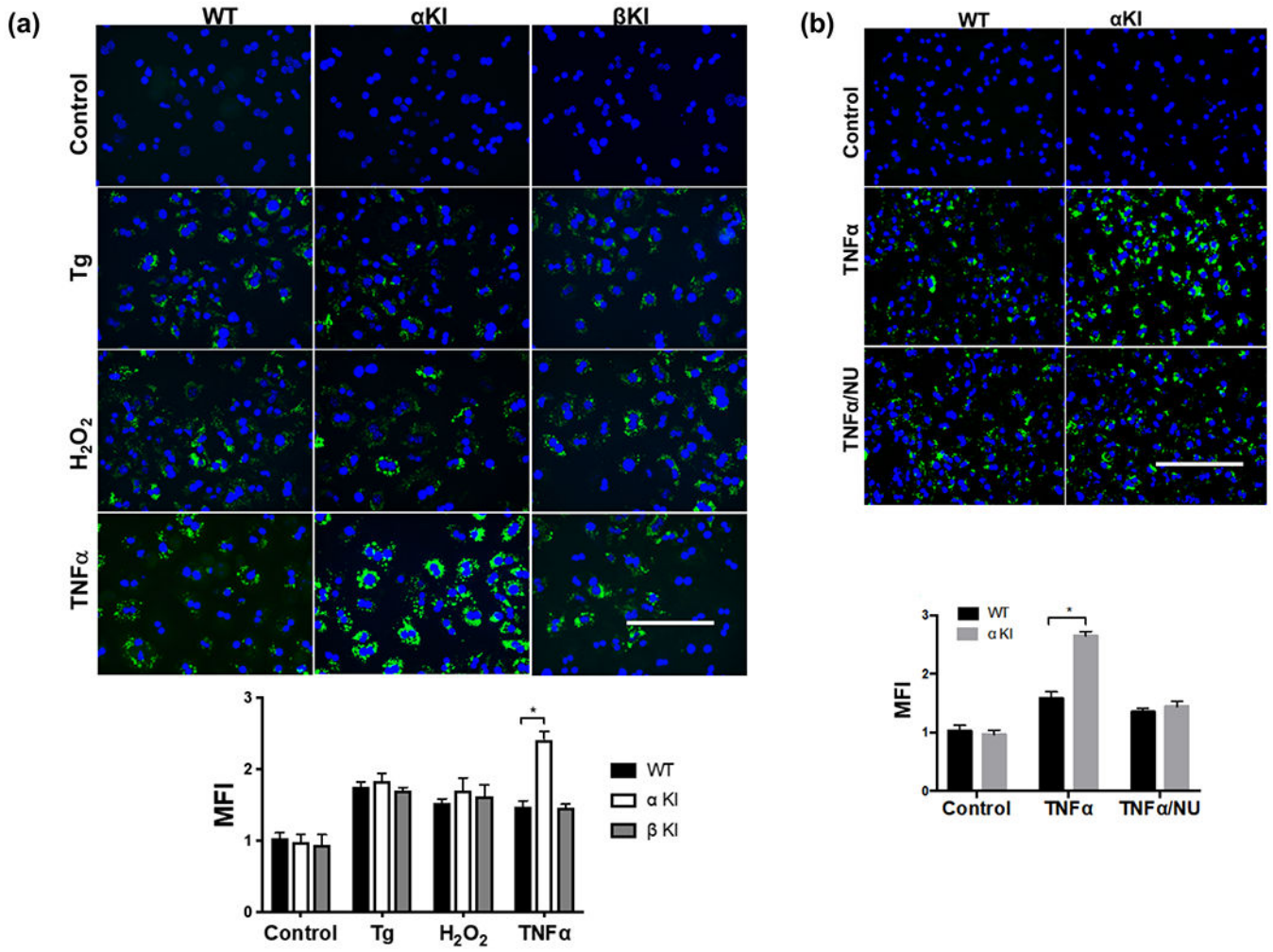

Figure 6:

Hepatocyte autophagy induction by TNF-a, oxidative and ER stress. Primary hepatocytes were isolated from WT and Gsk3α or β mutant KI mice. Autophagy was induced by ER stressor Thapsigargin (Tg) or H_2O_2 or TNF-a, as described in the Materials and Methods. Autophagy was detected by labeling cells with CYTO-ID® Green Detection Reagent. Cell nuclei were stained with DAPI. Labeled cells were analyzed by fluorescent microscopy. (a) Representative images of autophagic vacuoles in control- and stimulated- hepatocytes of WT and Gsk3α or β mutant. Mean fluorescent intensity (MFI) of different experimental groups were plotted. (b) Hepatocytes were incubated with TNF-α in the absence or presence of a TIP60 inhibitor NU9056 (NU). Autophagy vacuoles and cell nuclei were detected as above. Representative images and MFI of different experimental groups were shown. Representative results of 3 separate experiments. Scale bar=100μM, *p<0.05.

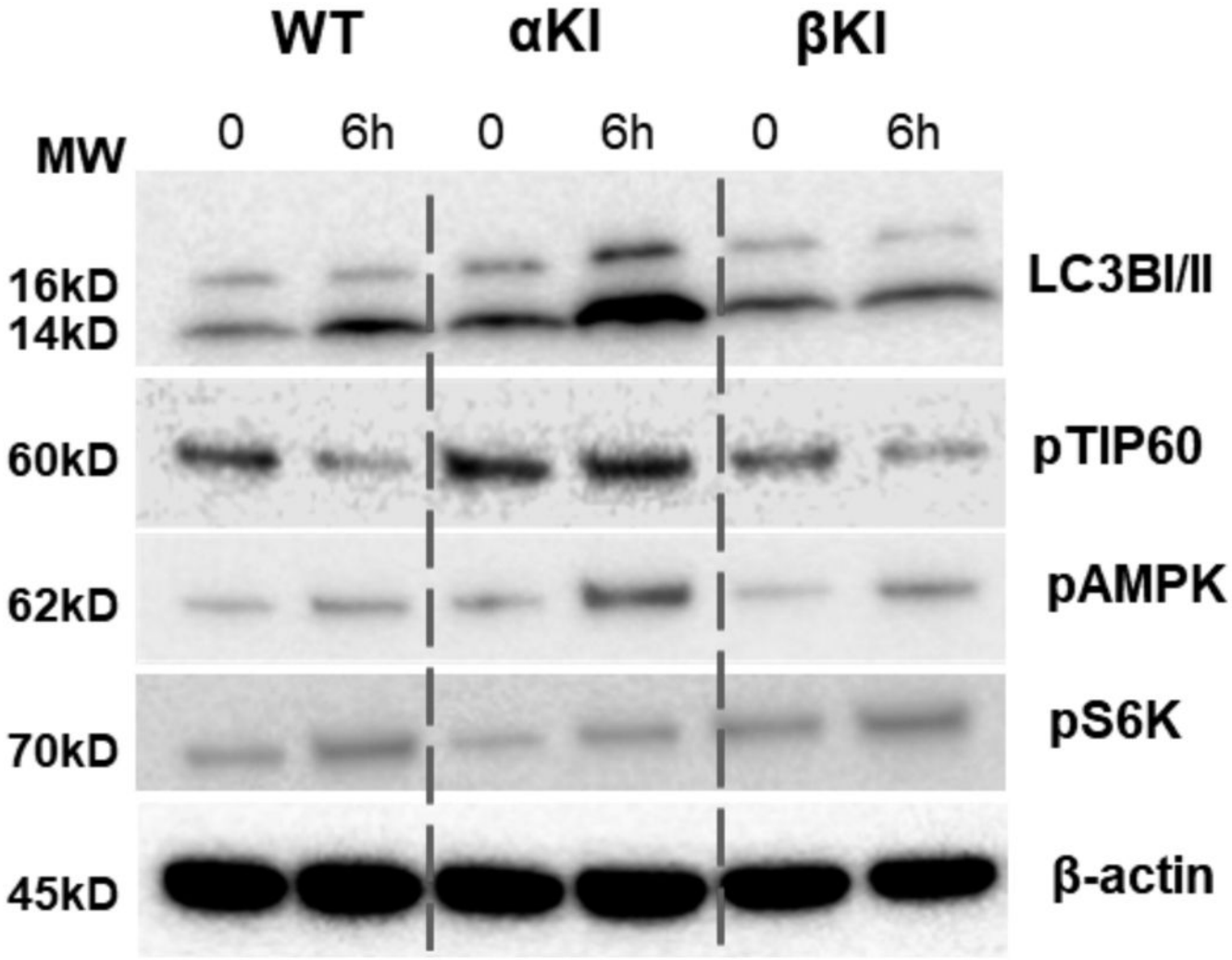

Figure 7:

Autophagy signaling pathways in liver IRI. WT and Gsk3α or β mutant KI mice were subjected to liver IR experiments, as described in the Materials and Methods. Sham and IR (harvested at 6h post reperfusion) livers were analyzed by Western blotting. Representative Western blots of phosphorylated forms of TIP60, AMPK, S6K and total LC3B I/II and β-actin. Representative results of 3 independent experiments.

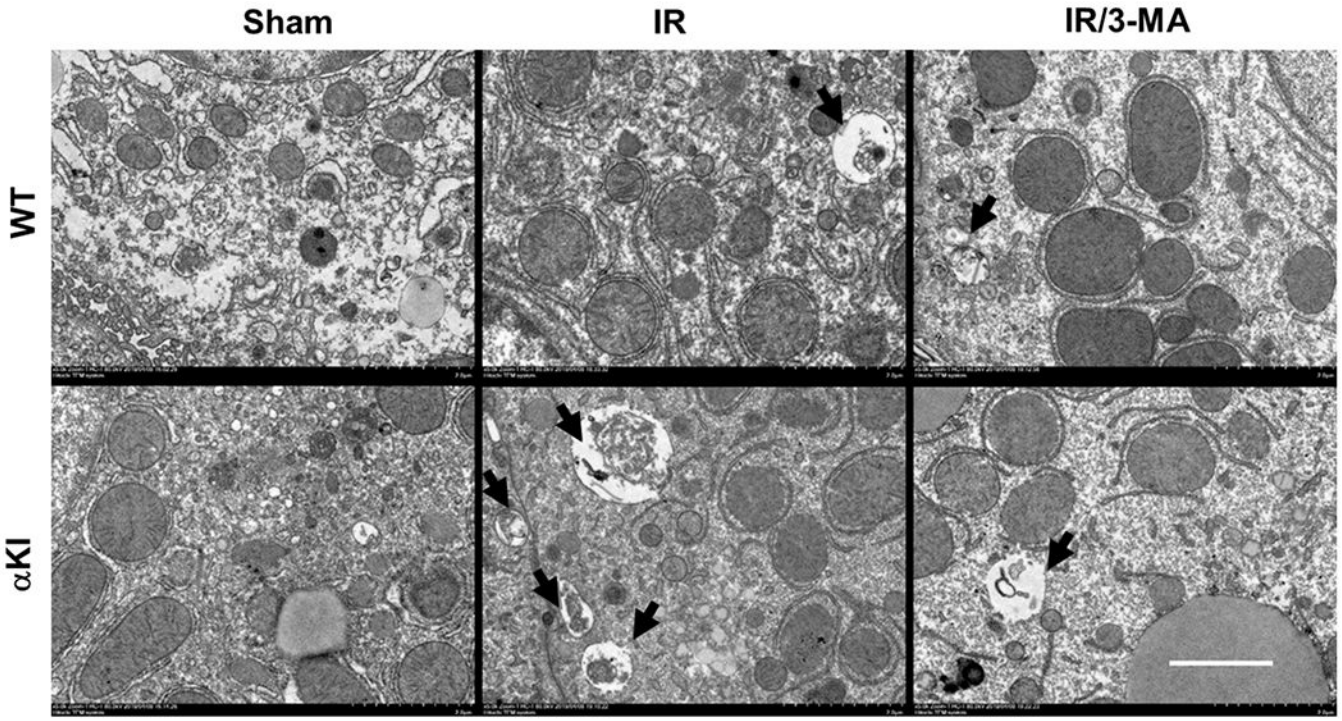

Figure 8:

Liver autophagy induction by IR. Tissue sections were prepared from either sham or IR livers in WT or Gsk3a mutant KI mice treated with or without 3-MA, as described in the Materials and Methods. Autophagosomes were detected by electron microscopy. Representative images of each experimental groups were shown. Scale bar=20μM.

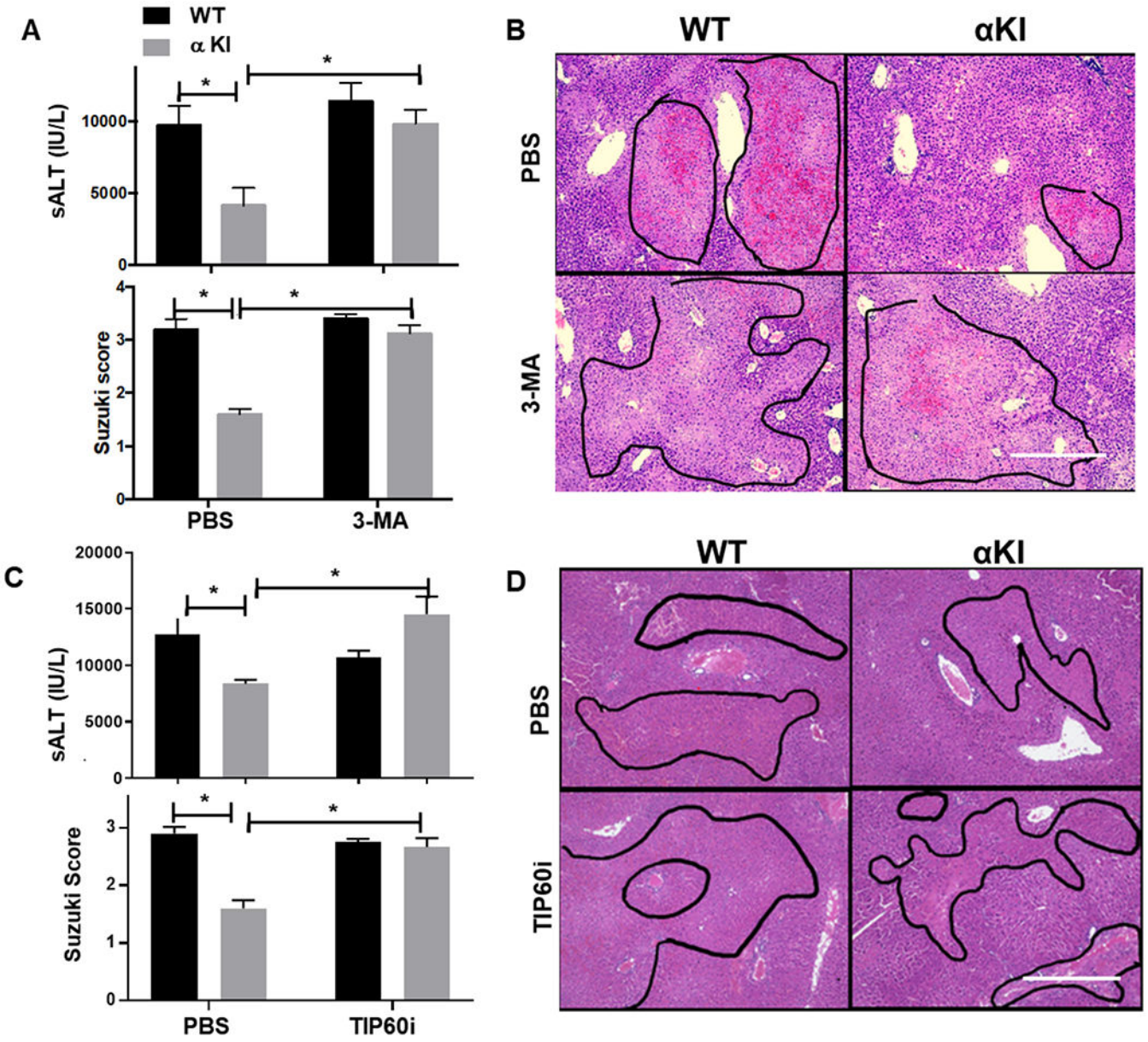

Figure 9:

Inhibition of autophagy or TIP60 increases liver IRI in Gsk3α mutant KI, but not WT mice. WT and Gsk3a mutant KI mice were pre-treated with 3-MA or TIP60 inhibitor TH1834 (TIP60i) prior to the onset of liver IR, as described in the Materials and Methods. Liver IRI was evaluated at 6h post reperfusion. (a, c) Average serum ALT levels and Suzuki scores, and (b, d) Representative liver histological pictures of different experimental groups were shown. Representative results of at least 2 experiments. Scale bar=200μM, *p<0.05.

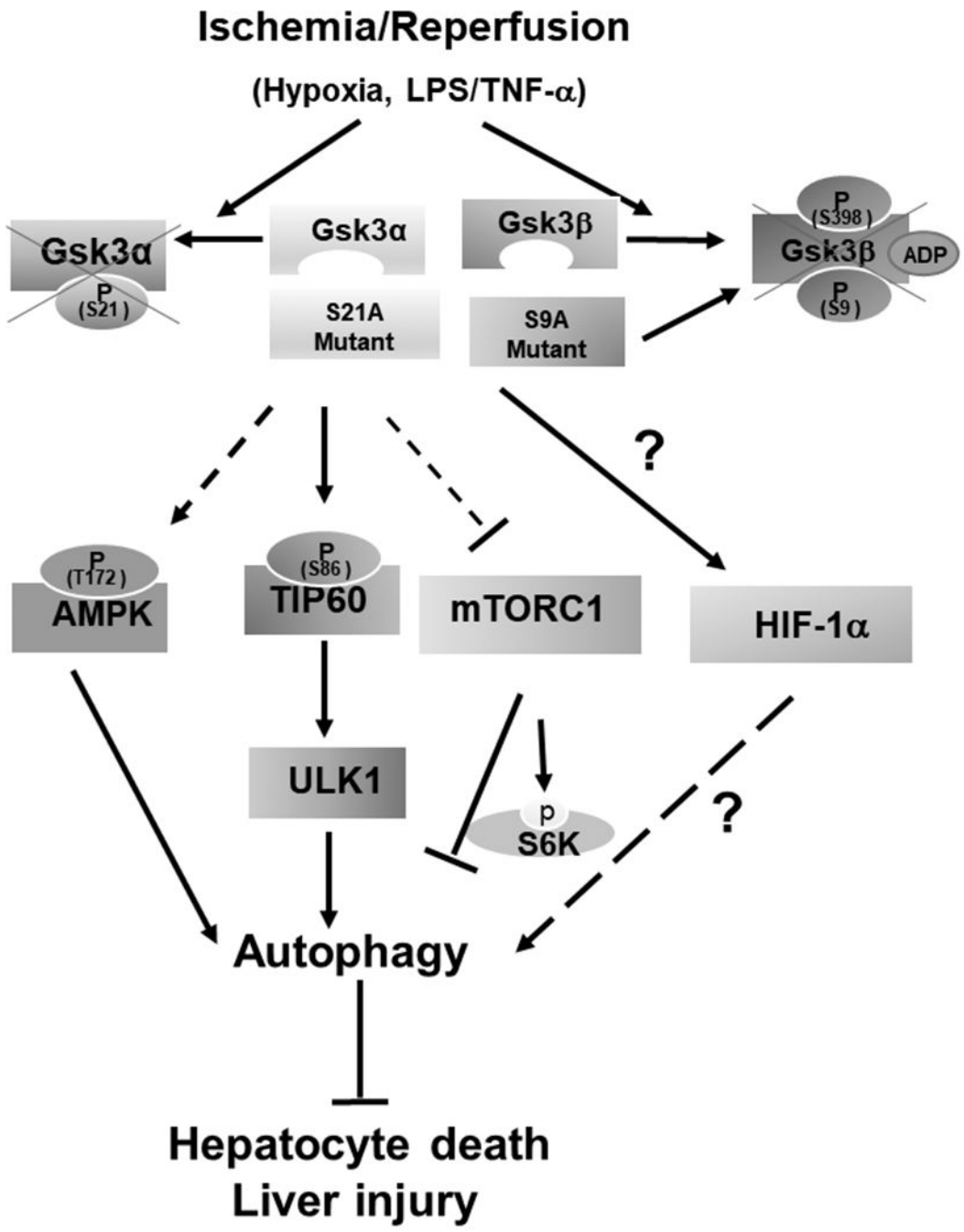

Figure 10.

Gsk3 regulates multiple intracellular signaling pathways in hepatocytes in response to IR. Hypoxia and inflammatory stimuli trigger the N-terminal inhibitory phosphorylation of Gsk3α/β during liver IR, leading to decreased activation of TIP60 (S86) and AMPKα (T172), increased activation of mTORC1, and possibly higher levels of HIF-1α. These pathways are involved in autophagy and pathogenesis of liver IRI. Gsk3α S21A mutation spares the kinase from this inhibitory phosphorylation and sustains its kinase activity, leading to higher TIP60, AMPK, and lower mTORC1 activation. Gsk3β S9A mutation,

on the other hand, is not sufficient to sustain its kinase activity in stimulation cells due to other inactivation mechanisms, e.g., S398 phosphorylation, ADP ribosylation, etc.